Association of brain network dynamics with plasma biomarkers in subjective memory complainers

Patrizia A. Chiesa [1,2,3,4], Marion Houot[2,5], Andrea Vergallo[1,2,3,4], Enrica Cavedo[1,2,3,4], Simone Lista[1,2,3,4] , Marie Claude Potier[6], Henrik Zetterberg[7,8,9,10], Kaj Blennow[7,8], Eugeen Vanmechelen[10], Ann De Vos[11], Bruno Dubois[2,3,4], and Harald Hampel[1,2,3,4]

and the INSIGHT-preAD study group

for the Alzheimer Precision Medicine Initiative (APMI)

1 AXA Research Fund & Sorbonne University Chair, Paris, France

2 Sorbonne University, GRC n° 21, Alzheimer Precision Medicine (APM), AP-HP, Pitié-Salpêtrière Hospital, Boulevard de l'hôpital, F-75013, Paris, France

3 Brain & Spine Institute (ICM), INSERM U 1127, CNRS UMR 7225, Boulevard de l'hôpital, F-75013, Paris, France

4 Institute of Memory and Alzheimer's Disease (IM2A), Department of Neurology, Pitié-Salpêtrière Hospital, AP-HP, Boulevard de l'hôpital, F-75013, Paris, France

5 Institute of Memory and Alzheimer's Disease (IM2A), Centre of excellence of neurodegenerative disease (CoEN), ICM, CIC Neurosciences, APHP Department of Neurology, Hopital Pitié-Salpêtrière, University Paris 6, Paris, France

6 Sorbonne Universités, UPMC Univ Paris 06, CNRS, INSERM, Laboratoire d'Imagerie Biomédicale, F-75013, Paris, France

7 Institute of Neuroscience and Physiology, Department of Psychiatry and Neurochemistry, The Sahlgrenska Academy at the University of Gothenburg, Mölndal, Sweden

8 Clinical Neurochemistry Laboratory, Sahlgrenska University Hospital, Mölndal, Sweden

9 Department of Neurodegenerative Disease, UCL Institute of Neurology, Queen Square, London, UK

10 UK Dementia Research Institute at UCL, London, UK

11 ADx NeuroSciences NV, Technologiepark 4, 9052, Ghent, Belgium

Abstract

Using a single integrated analysis, we examined the relationship between brain networks and molecular pathways in a cohort of elderly individuals at risk for Alzheimer's disease. In 205 subjective memory complainers (124 females, mean age: 75.7 ± 3.4), individual functional connectome was computed for a total of 3081 functional connections (set A) and 6 core plasma biomarkers of Alzheimer's disease (set B) were assessed. Partial least squares correlation analysis identified one dimension of population covariation between the 2 sets ($p < 0.006$), which we named bioneural mode. Five core plasma biomarkers and 190 functional connections presented bootstrap ratios greater than the critical value |1.96|. T-tau protein showed a trend toward significance (bootstrap resampling = 1.64). The salience, the language, the visuospatial, and the default mode networks were the strongest significant networks. We detected a strong association between network dynamics and core pathophysiological blood biomarkers. Innovative composite biomarkers, such as the bioneural mode, are promising to provide outcomes and better inform drug development and clinical practice for neurodegenerative diseases.

INTRODUCTION

Complex chronic diseases such as cancer, systemic immune diseases, diabetes, and neurodegenerative diseases exhibit a multi-factorial nature that originates from complex interactions among (epi)genomics, regulatory mechanisms, interactomics, synaptic dynamics, and environmental factors [1–3]. Such diseases – including Alzheimer's disease (AD) – may originate from progressive breakdown events (decompensation) occurring through molecular, cellular, synaptic, and large-scale brain networks [3]. During the earliest preclinical stages of AD , adaptive responses and compensatory mechanisms may be enhanced, thus preserving network functions and, ultimately, delaying progression to clinical onset [3–5].

Due to AD complexity, single investigational techniques cannot capture the accumulative converging and diverging system decompensations and failures that occur during the disease progression. A multi-modal approach seems more appropriate to elucidate the interaction between different AD-related pathophysiological mechanisms. In AD, genetic, age-related, and stressor-induced alterations lead to detrimental pathophysiological cascades, such as proteinopathies (i.e., misfolding and toxic accumulation of amyloid beta [Aβ] peptides and tau proteins), synaptic failure, loss of plasticity, neuroinflammation, immune-mediated responses, and neurodegeneration (i.e., neuronal dystrophy, cytoskeletal damage, and apoptosis) [3,6,7].

The diagnostic value of Aβ plaque and tau neurofibrillary tangle accumulation has led to investigations on the question whether and how these pathological hallmarks may affect large-scale brain function at different stages of the disease. There is accumulating evidence that amyloid pathology, as assessed by positron emission tomography (PET), is associated with significant disruptions of default mode network (DMN) connectivity in asymptomatic individuals [10–13], mild cognitive impairment (MCI) individuals [10], and AD dementia patients [10–12]. More recent studies investigated the relationship between functional network failure and cerebrospinal fluid (CSF) Aβ and tau concentrations [14–17]. Findings converge in providing evidence of reduced DMN integrity associated with low CSF $A\beta_{1-42}$ and high CSF tau concentrations [15,17]. According to Jones and colleagues [14], brain amyloid may mediate the association between brain network dysfunction and tau deposition. Indexes of disease severity originating from graph theory metrics showed disrupted DMN functional

connectivity in the presence of abnormal CSF biomarkers, suggesting that asymptomatic individuals at risk of AD may exhibit a milder AD network phenotype [16]. Besides these advances, little is known about the relationship between other molecular mechanisms and brain functional dynamics. Addressing these questions will reveal the true complexity of brain endophenotypes.

Here, we developed and used an integrative method that goes beyond the simple analysis of how biomarkers correlate with each connectome; we wanted to disclose whether any specific patterns of brain connectivity are associated with specific sets of biological fluid markers. In particular, we explored the *in vivo* the existence of an association between different molecular and brain network patterns in a cohort of asymptomatic individuals at risk for AD [18]. Data on brain functional dynamics and proteomics were gathered: functional network connectivity was assessed as a non-invasive biomarker for detection of early synaptic dysfunction in AD; while six core candidate blood-based biomarkers were selected based on their ability to identify distinctive AD-related pathophysiological mechanisms, such as brain proteinopathies, amyloidogenic pathways, neuroinflammation, and axonal damage. Peripheral biomarkers, compared to cerebrospinal fluid (CSF) and positron emission tomography (PET) markers, are increasingly gaining *momentum* due to their low cost, time effectiveness, and minimal invasiveness, which are meaningful aspects for healthcare and large-scale investigations and clinical trials [9,19].

METHODS

Participants

Data used in the preparation of this article were obtained from the "INveStIGation of AlzHeimer's PredicTors in Subjective Memory Complainers" (INSIGHT-preAD) study, a large-scale French mono-centric academic university-based observational cohort. Participants were enrolled at the Institute for Memory and Alzheimer's Disease (Institut de la Mémoire et de la Maladie d'Alzheimer, IM2A) at the Pitié-Salpêtrière University Hospital in Paris, France. The main purpose of the INSIGHT-preAD study is to investigate the earliest preclinical stages of AD and the dynamic development taking into account influencing factors and markers of progression [20].

The INSIGHT-preAD study includes 318 cognitively intact Caucasian older adults recruited from the community in the wider Paris area, France, aged 70 to 85, with subjective memory complaint (SMC), defined as follows: i) Participants answered "YES" to both questions «Are you complaining about your memory?» and «Is it a regular complaint that has lasted now more than 6 months?»; ii) Participants present intact cognitive functions based on the Mini-Mental State Examination (MMSE, ≥ 27), Clinical Dementia Rating scale (CDR, = 0), and Free and Cued Selective Rating Test (FCSRT, total score ≥ 41). The amyloid status, *APOE* genotype, demographic, cognitive, functional, nutritional, biological and genomic information, imaging, electrophysiological, and other assessments were determined at baseline. Written informed consent was provided by all participants. The study was approved by the local Institutional Review Board and was conducted in accordance with the Helsinki Declaration of 1975.

For the present study, we had considered only participants who underwent the resting state functional MRI (rs-fMRI) acquisition (n = 297) and for who biological data were available (n = 276), resulting in a sample size of 250 participants.

rs-fMRI data acquisition and preprocessing

Scanning was performed on a 3 Tesla MRI Scanner. During the rs-fMRI scan, participants were instructed to keep their eyes closed and stay as still as possible. The rs-fMRI images were collected by using an echo-planar imaging (EPI) sequence (TR = 2460 ms, TE = 30 ms, slice thickness = 3 mm, matrix = 64×64, voxel size = 3×3×3 mm^3, number of volumes = 250, number of slices = 45, run = 1) which is sensitive to blood oxygenation level–dependent (BOLD) contrast (T2* weighting). Only one rs-fMRI run was acquired for each participant.

The rs-fMRI data were preprocessed using Data Processing Assistant for Resting-State fMRI (DPARSF) [21] implemented in Data Processing & Analysis for Brain Imaging (DPABI, available at http://rfmri.org/dpabi), based on SPM8. The first 10 volumes for each participant were excluded to avoid potential noise related to the equilibrium of the magnet and participant's adaptation to the scanner. The remaining 240 volumes were preprocessed in a series of steps including slice-timing correction, realignment, and segmentation using SPM priors for CSF and white matter (WM). We

regressed out the global mean and the confounding effects of CSF and WM to reduce the effect of physiological noise. The Friston 24-parameter model, which includes six head motion parameters, six head motion parameters one time point before, and the 12 corresponding squared items, was used to regress out head motion effects [22]. A temporal band pass filtering (pass band 0.01–0.1 Hz) was applied to reduce the effect of low frequency drift and high frequency physiological noise.

The motion-corrected functional volumes were subsequently spatially normalized to the T1 unified segmentation template in Montreal Neurological Institute coordinates derived from SPM8 software and resampled to 3×3×3 mm3 voxels.

Functional connectomes

The objective of this analysis was to quantify functional connectivity in regions of interest (ROIs) included in networks previously shown to be involved in AD. Here, we selected networks that have hypothesized functions in AD-related pathology from the 14 networks defined by Shirer and colleagues [23] using independent-components analysis (available online at https://findlab.stanford.edu/functional_ROIs.html). Our selection included the anterior and posterior salience network (aSN and pSN, respectively), the ventral and dorsal default mode network (vDMN and dDMN, respectively), the Higher Visual Network (hVS), the Language Network (LN), the left and right Executive Control Network (LECN and RECN, respectively), the Sensorimotor Network (SN), the Precuneus Network (PN), the Visuospatial Network (VN). We excluded the auditory network, the primary visual network, and the sensorimotor network. In summary, our analyses included 79 brain functional ROIs, for a total of 3081 functional connections (edges) for each subject, according to the formula: (79 x 79 - 79) / 2.

The DPARSFA toolbox was used to create individual seed-to-seed connectivity maps including several steps. Firstly, the mean time series of each seed region was extracted and correlated (Pearson's correlation) with that of each other seed region. Then, the Fisher's r-to-z transform was applied to standardize the resulting correlation maps. Age, and MMSE score were included as covariates.

Blood sampling and collections tube storage

Blood samples were taken in the morning, after a 12-hour fast, handled in a standardized way, and centrifuged for 15 minutes at 2,000 G-force at 4°C. Per sample, plasma fraction was collected, homogenized, aliquoted into multiple 0.5 mL cryovial- sterilized tubes, and finally stored at -80°C within 2 hours from collection.

Plasma biomarkers assessment: additional description of the method

The concentration of the following candidate surrogate biomarkers were measured in plasma to assess: i) neurodegeneration and neurofibrillary pathology: t-tau, ii) brain amyloidosis: the 42 amino acid-long Aβ peptide ($A\beta_{1-42}$), the 40 amino acid-long Aβ peptide ($A\beta_{1-40}$), the related composite ratio $A\beta_{1-42}/A\beta_{1-40}$, and the β-site amyloid precursor protein cleaving enzyme 1 (BACE1), iii) glial activation and neuroinflammation: YKL-40, and iv) large caliber axonal damage: neurofilament light chain (NFL) protein.

Plasma $A\beta_{1-42}$ and $A\beta_{1-40}$ were analyzed using the Single molecule array (Simoa) immunoassay (Quanterix, Lexington, MA, USA). For $A\beta_{1-42}$, the repeatability was 4.1% and the intermediate precision was 7.0% for an internal QC plasma sample with a concentration of 10.5 pg/mL. Regarding $A\beta_{1-40}$, the repeatability was 4.0% and the intermediate precision was 6.4% for an internal QC plasma sample with a concentration of 203 pg/mL.

Plasma t-tau was measured using the Human Total Tau 2.0 kit on the Simoa platform (Quanterix, Lexington, MA). Plasma T-tau, both the repeatability and intermediate precision was 12.2% for an internal QC plasma sample with a concentration of 1.9 pg/mL [24]. Plasma NFL was measured using an in-house Simoa assay, as previously described in detail (ref: PMID: 26870824). Repeatability was 9.6% and 10.6% and intermediate precision was 14.6% and 11.6%, for two internal QC plasma samples with concentrations of 12.9 pg/mL and 107 pg/mL, respectively [24].

Plasma YKL-40 was analyzed using a commercial available ELISA kit (R&D Systems, Minneapolis, MN, US), according to manufacturer instructions[24]. Repeatability was 6.6% and 6.9% and intermediate precision 6.6% and 6.9%, for two internal QC plasma samples with concentrations of 14.100 pg/mL and 108.000 pg/mL.

Plasma BACE1 concentrations were measured at ADx NeuroSciences, Gent, Belgium, using a research prototype ELISA, based on the commercially available ELISA for CSF measurements (EQ 6541-9601-L; Euroimmun AG, Lübeck, Germany). The design of the CSF ELISA was previously described [25]. The intra-assay precision of this plasma research prototype was on average 2.1% CV and 3.2% CV (coefficient of variation), based on the two reference samples, run in duplicate and over 10 plates. The inter-assay variability was 8.5% CV and 9.5% CV (for more details see Supplementary material).

ADx401 (clone 5G7) coated plates were incubated simultaneously with the sample (15 µL; undiluted) and the biotinylated detector mAb ADx402 (clone 10B8F1), for three hours at room temperature. For plasma measurements, the same protocol as that for the CSF analysis was used, as instructed by the manufacturer. Additionally, the same material of the CSF kit was used, including the lyophilized, ready-to-use calibrators and run validation controls. The only modification involved the buffer of the biotinylated detector mAb, which was diluted in a buffer adapted for the plasma matrix and contained a heterophilic blocker reagent. After analysis, BACE1 concentrations were calculated via intrapolation (5PL curve fit; log (X)) based on the calibrator curve. In parallel to the clinical plasma samples, which were blinded and randomized before testing, two reference samples from ADx NeuroSciences were analyzed.

Statistical analyses

We aimed to relate functional connectomes to AD-relevant plasma biomarkers in an integrated analysis. To this aim, we applied the Partial Least Squares Correlation (PLSC), a procedure that seeks maximal correlations between combinations of variables in two sets [26]. The 3,081 connectomes were combined into a single large connectome matrix (set A) containing all connectomes (in columns) for all subjects (in lines). The six blood-based biomarkers (BACE1, $A\beta_{1-42}$, the $A\beta_{1-40}/A\beta_{1-42}$ ratio, tau, NFL, and YKL-40) were included in a separated matrix (set B). The goal was to find the shared information between these two sets. For this purpose, singular value decomposition was applied on the covariance matrix between both sets. Thus, new variables for each set (called latent variables) were calculated as linear combination of the original variables with the singular vectors for each dimension

which maximized covariance between both variables.

Statistical significance of PLSC was assessed by resampling methods: the significance of the global model and the dimensions were assessed with permutation tests (we used 10,000 permuted samples); whereas the significance of specific measures of each set in a dimension was assessed via the Bootstrap [27]. Bootstrap ratios were computed by dividing the weight of a variable by the standard deviation of its bootstrapped distribution. The bootstrap ratio is akin to a Student t criterion and the absolute value of 1.96 roughly corresponds to the critical value $\alpha = .05$ [28].

Absolute values of blood biomarkers and connectomes higher than seven standard deviations of the mean were excluded from the analysis. Age, sex, and *APOE ε4* were regressed out of biological markers data as potential confounding factors, as well as sex, total intracranial volume and *APOE ε4* for connectomes.

Statistical analyses were performed using R version 3.3.2 (available at https://www.r-project.org).

RESULTS

Participants

Eleven of the 250 participants did not qualify for the fMRI analyses due to incidental imaging abnormalities (ten had a meningioma, and one did not conclude the entire rs-fMRI acquisition). Thirty-four additional participants were excluded because absolute values of blood biomarkers or connectomes were seven standard deviations higher than the mean.

Demographic characteristics, global cognition, biological measures, and *APOE* genotype of the final subset of 205 participants are shown in Table 1.

Partial least squares correlation (PLSC) analysis

Using PLSC, we estimated the relationship between plasma biomarkers and the functional brain dynamics at rest. PLSC identify pairs of variates along which sets of plasma biomarkers that are related to the AD pathophysiology and patterns of brain connectivity co-varying in a similar way across participants (bio-neural mode). This analysis revealed a single highly significant component that relates functional connectomes to biological measures (Component 2, Cov = 965.9, p = .006).

Such component explained around the 21% of the total covariance. The relationships of all participants with this mode, i.e., individual scores in the plasma surrogate biomarkers *versus* individual scores in the connectome correlation, are also plotted in Figure 1: high-scoring subjects (top-right points in the scatter-plot) have high relative values for both brain functional and plasma biomarker values.

Figure 2 displays the strength of association of the 6 plasma biomarkers with the significant PLSC mode. Interestingly, all the bootstrap ratios of the blood-based surrogate biomarkers were negative.

190 connectomes were significant. In particular, the salience networks the DMN, and the language and executive control networks were the most represented among the significant connectomes (Figure 3).

Discussion

Unravelling the link across different multi-scale systems during the earliest stages of AD is critical to understand the complex pathophysiological dynamics of the evolving underlying disease. We applied an integrated analysis on brain imaging and fluid biomarkers of AD within a cohort of elderly individuals at risk for AD.

We found one combination of variables composed by blood-based biomarkers and functional connectomes that maximally co-varied among individuals at risk for AD (i.e., mode). These results confirm previous findings showing the existence of a synergistic relationship between network failure and pathophysiological fluid biomarkers [14–17]. However, our results boost previous findings showing that different pathophysiological mechanisms – including brain proteinopathies, neuroinflammation, axonal damage, and neurodegeneration – emerge in aging asymptomatic at-risk individuals for AD. In the present study, none of the plasma biomarkers of the selected comprehensive panel had a significant comparative performance; instead, all analysed molecular biomarkers seem to contribute to the unified analysis, and affect neural networks. Such evidence agrees with the manifold pathomechanistic alterations occurring in AD and with the hypothesis that a single molecular biomarker i) cannot account for the complexity of the molecular landscape of AD, and ii) is not sufficient to generate substantial predictive power. It is also worthwhile highlighting that all the biological markers correlate negatively with the significant mode. A previous study used a similar method to evaluate the correlation between behavioural and imaging measures [29]. Authors identified a "positive-negative" axis, where positively correlated behavioral indexes are commonly considered as positive personal qualities (e.g., life satisfaction, years of education, income), and negatively behavioral indexes relate to negative traits (e.g., those related to substance use, rule breaking behavior, anger). Following the same interpretation, our analysis may reveal that all the selected fluid biomarkers may be related to pathological conditions.

In contrast, the overall connectome-modulation latent variables and the original connectomes are positively inter-correlated, as indicated by the dominance of red-coloured edges reported in Figure 3. These results denote that individuals scoring highly in the bio-neural mode demonstrate increased

concentrations of molecular biomarkers and stronger overall connectivity than low-scoring individuals. The emerging connectivity pattern involves, but is not limited to, the salience networks, the DMN, and the language and executive control networks. Findings are converging in identifying alterations in these networks throughout the temporal AD continuum [30,31]. However, only DMN dysfunctions related to decreased CSF $A\beta_{1-42}$ and high CSF total tau concentrations have been investigated and demonstrated so far [15,17].

In the context of complex and non-linear dynamic diseases, such as AD, spatio-temporal changes may gradually breakout across brain networks, leading to widespread disconnections and progressive cognitive dysfunctions. However, the mechanisms underlying the dynamic spreading of pathophysiological mechanisms are not yet fully elucidated [32].

Identifying key brain regions that are more vulnerable to stressors is a relevant information regarding expected treatment effects on brain function. Using these regions as disease outcomes during early stages could reflect effects on adaptive responses and compensatory mechanisms, preserving brain homeostasis before the spreading of any AD-related pathophysiological mechanisms. The question of how homeostasis can be preserved through dynamic adaptive responses and compensatory mechanisms occurring across molecules, cells, and higher complexity networks needs further elucidation.

We hypothesize that the identified bio-neural mode might represent a promising innovative composite biomarker to track *in vivo* the dynamic interplay between molecular mechanisms and network organizational patterns related to AD pathophysiology. The present study involved individuals at risk of developing AD and, thus, may support the hypothesis of strong interindividual variability in adaptive responses and compensatory mechanisms ensuring brain and body homeostasis [3,33–36]. Long-term follow-up studies, including a sufficient number of progressors to symptomatic stages, are necessary to clarify whether the bio-neural mode may correspond to adaptive/compensatory dynamics. In our opinion, the bio-neural mode may be informative as an outcome of drug trials in Research & Development (R&D) programs for putative disease-modifying compounds [3,37,38].

Composite biomarkers, such as the bio-neural mode, may contribute to the development of systems pharmacology-based approaches in drugs Research & Development (R&D) programs [2,38,39]. Systems

pharmacology can predict both the effect and the safety profile of drugs across biological networks and body systems computing the inter-individual genetic and biological variability [2,38,39]. Pursuing this approach will translate into the accomplishment of the precision pharmacology which represent a paradigm shift in decision-making processes for drug R&D programs which develop pathway-based therapies individually tailored to a biological staging workflow [3,40]. Precision pharmacology, presently evolving in more advanced areas of medicine, such as oncology [41], is expected to promote the development in the field of neurodegenerative diseases, including AD, in line with the framework of precision medicine.

Acknowledgements

HZ is a Wallenberg Academy Fellow supported by grants from the Swedish Research Council, the European Research Council and the UK Dementia Research Institute at UCL.

References (< 50 references)

1. Bassett, D. S. & Sporns, O. Network neuroscience. *Nat. Neurosci.* **20,** 353–364 (2017).
2. Harrold, J. M., Ramanathan, M. & Mager, D. E. Network-based approaches in drug discovery and early development. *Clin. Pharmacol. Ther.* **94,** 651–658 (2013).
3. Hampel, H. *et al.* Precision pharmacology for Alzheimer's disease. *Pharmacol. Res.* **130,** 331–365 (2018).
4. Stern, Y. *et al.* Different brain networks mediate task performance in normal aging and AD: Defining compensation. *Neurology* **55,** 1291–1297 (2000).
5. Arenaza-Urquijo, E. M. & Vemuri, P. Resistance vs resilience to Alzheimer disease: Clarifying terminology for preclinical studies. *Neurology* **90,** 695–703 (2018).
6. Bokde, A. L. W., Ewers, M. & Hampel, H. Assessing neuronal networks: Understanding Alzheimer's disease. *Prog. Neurobiol.* **89,** 125–133 (2009).
7. Selkoe, D. J. Alzheimer's disease is a synaptic failure. *Science* **298,** 789–791 (2002).
8. Bokde, A. L. W., Ewers, M. & Hampel, H. Assessing neuronal networks: Understanding Alzheimer's disease. *Prog. Neurobiol.* **89,** 125–133 (2009).
9. Hampel, H. *et al.* Blood-based biomarkers for Alzheimer disease: mapping the road to the clinic. *Nat. Rev. Neurol.* **14,** 639–652 (2018).
10. Drzezga, A. *et al.* Neuronal dysfunction and disconnection of cortical hubs in non-demented subjects with elevated amyloid burden. *Brain* **134,** 1635–1646 (2011).
11. Mormino, E. C. *et al.* Relationships between Beta-Amyloid and Functional Connectivity in Different Components of the Default Mode Network in Aging. *Cereb. Cortex* **21,** 2399–2407 (2011).
12. Sheline, Y. I. *et al.* Amyloid Plaques Disrupt Resting State Default Mode Network Connectivity in Cognitively Normal Elderly. *Biol. Psychiatry* **67,** 584–587 (2010).
13. Hedden, T. *et al.* Disruption of Functional Connectivity in Clinically Normal Older Adults Harboring Amyloid Burden. *J. Neurosci.* **29,** 12686–12694 (2009).
14. Jones, D. T. *et al.* Tau, amyloid, and cascading network failure across the Alzheimer's disease spectrum. *Cortex* **97,** 143–159 (2017).
15. Palmqvist, S. *et al.* Earliest accumulation of β-amyloid occurs within the default-mode network and concurrently affects brain connectivity. *Nat. Commun.* **8,** 1214 (2017).
16. Brier, M. R. *et al.* Functional connectivity and graph theory in preclinical Alzheimer's disease. *Neurobiol. Aging* **35,** 757–768 (2014).
17. Wang, L. *et al.* Cerebrospinal Fluid Aβ42, Phosphorylated Tau 181 , and Resting-State Functional Connectivity. *JAMA Neurol.* **70,** 1242–1248 (2013).
18. Dubois, B. *et al.* Cognitive and neuroimaging features and brain β-amyloidosis in individuals at risk of Alzheimer's disease (INSIGHT-preAD): a longitudinal observational study. *Lancet Neurol.* **17,** 335–346 (2018).
19. O'Bryant, S. E. *et al.* Blood-based biomarkers in Alzheimer disease: Current state of the science and a novel collaborative paradigm for advancing from discovery to clinic. *Alzheimers. Dement.* **13,** 45–58 (2017).
20. Dubois, B. *et al.* Cognitive and neuroimaging parameters and brain amyloidosis in individuals at risk of Alzheimer's disease (INSIGHT-preAD): a longitudinal observational study. *Lancet Neurol.* **in press,** (2018).
21. Yan, C.-G., Wang, X.-D., Zuo, X.-N. & Zang, Y.-F. DPABI: Data Processing & Analysis for (Resting-State) Brain Imaging. *Neuroinformatics* **14,** 339–351 (2016).
22. Friston, K. J., Williams, S., Howard, R., Frackowiak, R. S. & Turner, R. Movement-related effects in fMRI time-series. *Magn. Reson. Med.* **35,** 346–55 (1996).

23. Shirer, W. R., Ryali, S., Rykhlevskaia, E., Menon, V. & Greicius, M. D. Decoding Subject-Driven Cognitive States with Whole-Brain Connectivity Patterns. *Cereb. Cortex* **22,** 158–165 (2012).
24. Olsson, B. *et al.* CSF and blood biomarkers for the diagnosis of Alzheimer's disease: a systematic review and meta-analysis. *Lancet. Neurol.* **15,** 673–684 (2016).
25. De Vos, A. *et al.* The Cerebrospinal Fluid Neurogranin/BACE1 Ratio is a Potential Correlate of Cognitive Decline in Alzheimer's Disease. *J. Alzheimers. Dis.* **53,** 1523–1538 (2016).
26. Krishnan, A., Williams, L. J., McIntosh, A. R. & Abdi, H. Partial Least Squares (PLS) methods for neuroimaging: A tutorial and review. *Neuroimage* **56,** 455–475 (2011).
27. Efron, B. & Tibshirani, R. *Bootstrap Methods for Standard Errors, Confidence Intervals, and Other Measures of Statistical Accuracy*. *Statistical Science* **1,** (1986).
28. Abdi, H. & Williams, L. J. in 549–579 (2013). doi:10.1007/978-1-62703-059-5_23
29. Smith, S. M. *et al.* A positive-negative mode of population covariation links brain connectivity, demographics and behavior. *Nat. Neurosci.* **18,** 1565–1567 (2015).
30. Pievani, M., Filippini, N., van den Heuvel, M. P., Cappa, S. F. & Frisoni, G. B. Brain connectivity in neurodegenerative diseases—from phenotype to proteinopathy. *Nat. Rev. Neurol.* **10,** 620–633 (2014).
31. Pievani, M., de Haan, W., Wu, T., Seeley, W. W. & Frisoni, G. B. Functional network disruption in the degenerative dementias. *Lancet Neurol.* **10,** 829–843 (2011).
32. Fornito, A., Zalesky, A. & Breakspear, M. The connectomics of brain disorders. *Nat. Rev. Neurosci.* **16,** 159–172 (2015).
33. Apostolova, I. *et al.* Hypermetabolism in the hippocampal formation of cognitively impaired patients indicates detrimental maladaptation. *Neurobiol. Aging* **65,** 41–50 (2018).
34. Perez-Nievas, B. G. *et al.* Dissecting phenotypic traits linked to human resilience to Alzheimer's pathology. *Brain* **136,** 2510–2526 (2013).
35. Elman, J. A. *et al.* Neural compensation in older people with brain amyloid-beta deposition. *Nat. Neurosci.* **17,** 1316–1318 (2014).
36. Krishnan, V. *et al.* Molecular adaptations underlying susceptibility and resistance to social defeat in brain reward regions. *Cell* **131,** 391–404 (2007).
37. Cummings, J., Ritter, A. & Zhong, K. Clinical Trials for Disease-Modifying Therapies in Alzheimer's Disease: A Primer, Lessons Learned, and a Blueprint for the Future. *J. Alzheimers. Dis.* **64,** S3--S22 (2018).
38. Zhao, S. & Iyengar, R. Systems pharmacology: network analysis to identify multiscale mechanisms of drug action. *Annu. Rev. Pharmacol. Toxicol.* **52,** 505–521 (2012).
39. Geerts, H., Spiros, A., Roberts, P. & Carr, R. Quantitative systems pharmacology as an extension of PK/PD modeling in CNS research and development. *J. Pharmacokinet. Pharmacodyn.* **40,** 257–265 (2013).
40. Hampel, H. *et al.* Revolution of Alzheimer Precision Neurology. Passageway of Systems Biology and Neurophysiology. *J. Alzheimers. Dis.* **64,** S47–S105 (2018).
41. Drilon, A. *et al.* Efficacy of Larotrectinib in TRK Fusion-Positive Cancers in Adults and Children. *N. Engl. J. Med.* **378,** 731–739 (2018).

Figures and Tables

Variable	All	APOE e4-	APOE e4+	p - value
Participants	205	163 (80%)	42 (20%)	
Female	124 (60%)	95 (58%)	29 (69%)	.203
Male	81 (40%)	68 (42%)	13 (31%)	
Age (yrs)	75.7 ± 3.4	75.7 ± 3.4	75.6 ± 3.4	.830
MMSE	28.7 ± 1.0	28.7 ± 1.0	28.6 ± 1.0	.323
YKL40	58818.9 ± 40913.5	60093.9 ± 43113.7	53870.6 ± 30865.8	.381
NFL	29.7 ± 12.6	29.5 ± 13.1	30.5 ± 10.0	.664
Tau	4.5 ± 2.2	4.6 ± 2.3	4.3 ± 1.7	.435
Aβ42	18.4 ± 5.2	18.9 ± 5.4	16.2 ± 3.8	.003*
Ratio4240	.06 ± .01	.06 ± .01	.05 ± .01	.002*
BACE1	1109.2 ± 189.8	1104.0 ± 190.6	1129.4 ± 187.4	.441

* p < .05 t-test

MMSE = Mini Mental State Examination; YKL40 =Chitinase-3-like protein 1; NFL = neurofilament light protein; Aβ = amyloid beta peptide; BACE1 = Beta-secretase 1

Table 1. Demographic, neuropsychological, and biological measures. Counts, percentages, means, and standard deviations are shown for the two groups, as well as p-values, to indicate statistically significant group differences. T-test was performed for continuous variables and chi-square test for categorical variables.

MMSE = Mini-Mental State Examination; YKL40 = Chitinase-3-like protein 1; NFL = neurofilament light protein; Aβ = amyloid beta peptide; BACE1 = β-site amyloid precursor protein cleaving enzyme 1.

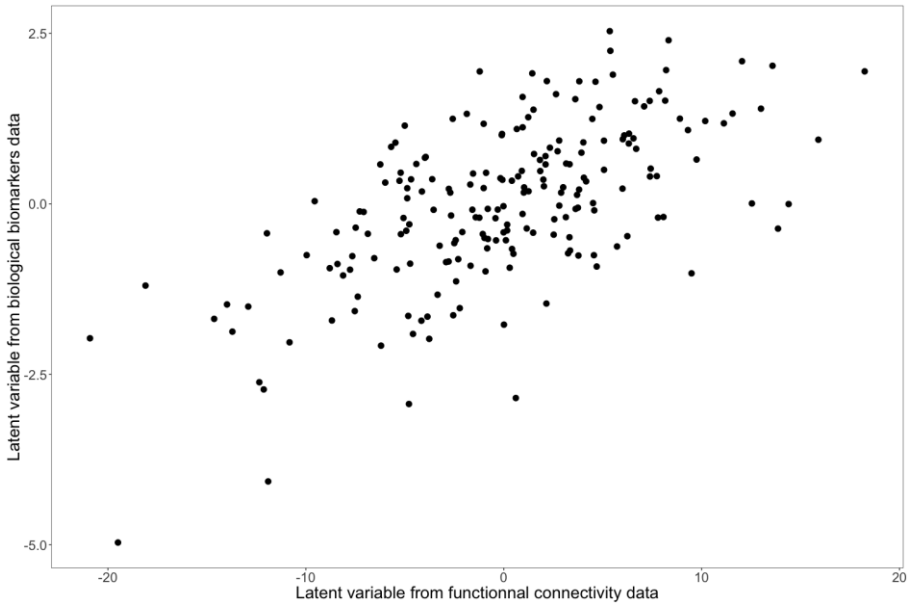

Figure 1. The scatter-plot represents the bio-neural mode: plasma biomarkers latent variables *versus* connectome latent variables are shown for each individual. The high correlation represented indicates significant co-variation between the two datasets, i.e. plasma biomarkers and brain functional connectomes.

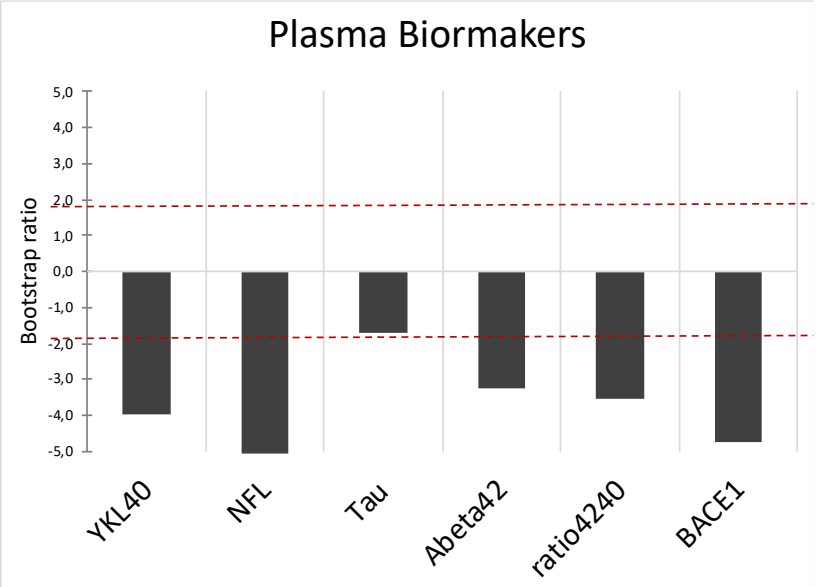

Figure 2. Association strength of plasma biomarkers. The six plasma biomarkers are strongly associated with the PLSC significant component (BR ≥ 1.96). Note: BR = bootstrap ratio.

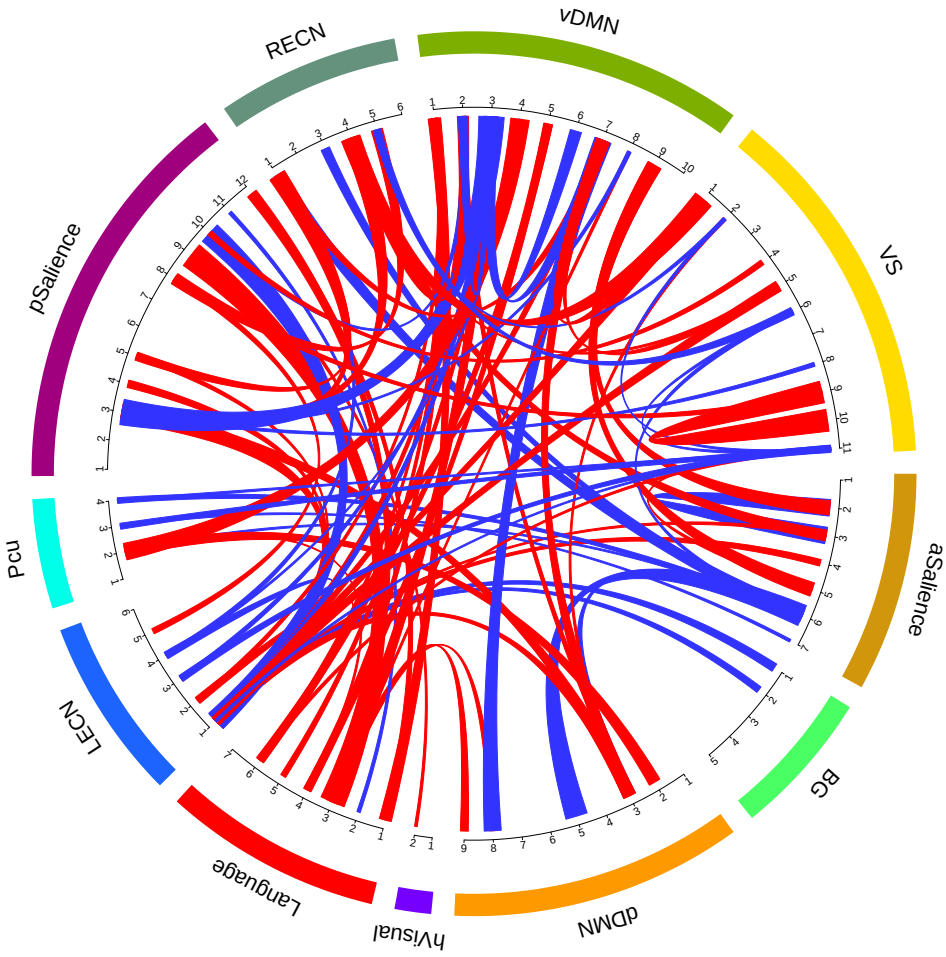

Figure 3. The 190 brain connections associated with the PLSC bio-neural mode. Red indicates positive connections; blue indicates negative connections. The thickest curves represent connections with largest PLSC weights. RECN = right executive control network; vDMN= ventral default mode network; VS = visual spatial network; aSalience = anterior salience network; BG = basal ganglia network; dDMN = dorsal default mode network; hVisual = high visual networks; Language = Language network; LECN = left executive control network; Pcu = precuneus network; pSalience = posterior salience network.